Radar measurements of the axis ratios of cloud particles

Valery Melnikov and Sergey Matrosov+*

*CIMMS, University of Oklahoma, Norman OK. +-CIRES University of Colorado and NOAA Earth Science Research Laboratory, Boulder, CO.

Theoretical basis for estimations of the axis ratios

The Circular Depolarization Ratio (CDR) depends upon the axis ratio (b/a) of a particle and is relatively weakly affected by its orientation (angles θ and φ in Fig. 1) for lower radar elevations. CDR can be used for estimating the axis ratio. CDR is measured by radars that employ circular polarization measurement scheme.

The most popular radar polarization scheme now is one with Simultaneous Transmission And Reception (STAR) of horizontally and vertically polarized waves. For a STAR radar, it is possible to derive a measurable that is a proxy of CDR.

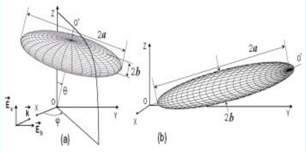

Fig. 1. Scattering geometry for plate-like (a) and columnar (b) particles. E_h and E_v are the electric vectors of incidence radiation. Angles *θ* and *φ* are orientation angles of a particle. Angle *θ* is the true canting angle.

CDR can be expressed via elements of the amplitude scattering matrix S_{hh} and S_{vv}:

$$CDR=10\log_{10}(<|S_{hh}-S_{vv}|^2>/<|S_{hh}+S_{vv}|^2>) \quad (1)$$

CDR in linear units can be expressed as

$$CDR=\frac{<|E_{hr}-E_{vr}|^2>}{<|E_{hr}+E_{vr}|^2>}=\frac{P_h+P_v-2\,\mathrm{Re}(R_{hv})}{P_h+P_v+2\,\mathrm{Re}(R_{hv})} \quad (2)$$

E_{hr} and E_{vr} are received voltages on the horizontal and vertical polarizations, $P_{h,v}$ are corresponding powers, and R_{hv} is the copolar correlation function

A STAR radar receives voltages which are given by:

$$\begin{pmatrix}E_{hr}\\E_{vr}\end{pmatrix}=C\begin{pmatrix}1 & 0\\0 & \exp[i(\psi_r+\frac{1}{2}\Phi_{dp})]\end{pmatrix}\begin{pmatrix}S_{hh} & S_{hv}\\S_{hv} & S_{vv}\end{pmatrix}\begin{pmatrix}1 & 0\\0 & \exp[i(\psi_t+\frac{1}{2}\Phi_{dp})]\end{pmatrix}\begin{pmatrix}E_h\\E_v\end{pmatrix}, \quad (3)$$

where Φ_{dp} is the scattering medium differential phase, Ψ_t and Ψ_r are the radar differential phases upon transmission and reception.

Substitution E_{hr} and E_{vr} from eq. (3) into eq. (2) and replacing $\mathrm{Re}(R_{hv})$ with $|R_{hv}|$, provides a proxy for intrinsic CDR (hereafter called SDR):

$$SDR=\frac{P_h+P_v-2|R_{hv}|}{P_h+P_v+2|R_{hv}|}=\frac{Z_{dr}+1-2Z_{dr}^{1/2}\rho_{hv}}{Z_{dr}+1+2Z_{dr}^{1/2}\rho_{hv}} \quad (4)$$

Modeling

By expressing P_h, P_v, and R_{hv} via polarizabilities α_a and α_b along the main particle's axes, SDR is expressed as,

$$SDR=\frac{<|\Delta\alpha|^2>A}{4<|\alpha_a|^2>+2\,\mathrm{Re}<(\alpha_a\Delta\alpha^{2})>B+<|\Delta\alpha|^2>C} \quad (5)$$

$$A=1-3J_1+J_1^2+11J_2/8 \qquad B=2-J_1 \qquad C=1-J_1-J_1^2+11J_2/8$$

$$\Delta\alpha=\alpha_b-\alpha_a, \qquad J_1=<\sin^2\theta>, \qquad J_2=<\sin^4\theta>.$$

where J_1 and J_2 are depend on the intensity of fluttering σ_θ; the brackets stand for angular averaging. Polarizabilities depend upon *b/a* and particle complex refractive index that makes it possible to estimate *b/a* from SDR.

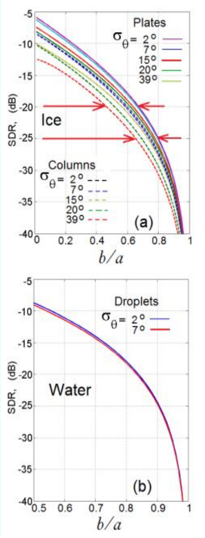

Fig. 2. SDR as a function of axis ratio *b/a* for different solid ice particles (a) and water drops (b) and for different fluttering magnitudes σ_θ.

The Fisher distribution for canting angles *θ* was used here:

$$p(\theta)=\frac{\mu}{2\sinh(\mu)}\exp(\mu\cos\theta)$$

where $\mu=\mu(\sigma_\theta)$ is a parameter that depends on the canting angle standard deviation σ_θ, which characterizes the flutter intensity of particles. A value of σ_θ=2° corresponds to particles with major dimensions oriented mostly in the horizontal plane and σ_θ=39° corresponds to particles that are oriented almost randomly in space.

It is seen from Fig. 2a that SDR depends upon the particle type (plates or columns), the axis ratio, and the magnitude of fluttering σ_θ. The main contributor is the axis ratio b/a. This is used to estimate *b/a* from SDR calculated from (4) using STAR mode radar measurables. For instance, if SDR is -20 dB, then *b/a* is in an interval from 0.45 to 0.70 (the upper red arrows in Fig. 2a) for any particle type and fluttering magnitude. If SDR values are less than -20 dB, this uncertainty is smaller: for SDR = -25 dB, the interval is 0.65 < *b/a* < 0.80 (the lower red arrows in Fig. 2a), which is a good estimate for the axis ratio. For SDR = -15 dB, the corresponding axis ratio interval is 0.2 < *b/a* < 0.5.

SDR is immune to Φ_{DP} in contrast to CDR. Z_{DR} is affected by differential attenuation A_{dp}. The impact of A_{dp} on SDR is much smaller compared to Z_{DR} because A_{dp} enters in the nominator and denominator of eq. (4). Thus the propagation effects should be less pronounced in SDR fields than in Z_{DR} fields. This fact is demonstrated using observational data (Fig. 4).

Observational data

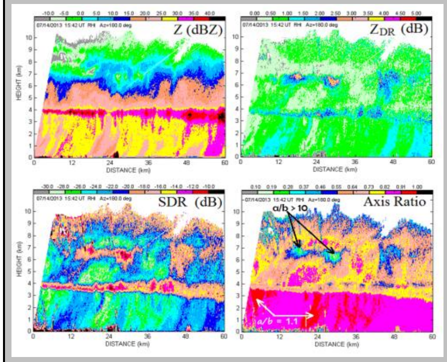

Fig. 3. (left top): Vertical cross-section of reflectivity observed on 14 July, 2013 at 1542Z at an azimuth of 180° (left right, low left, and low right frames correspond to Z_{DR}, SDR, and Axis Ratio (b/a) fields. The Axis Ratio field was generated from the SDR field using eq. (5). Note areas with particles having a/b > 10; the areas are shown with black arrows. Note also areas of a/b about 1 shown with the white arrows (the left lower corner of the Axis Ratio panel). So SDR indicates particle axis ratios varying in a wide interval.

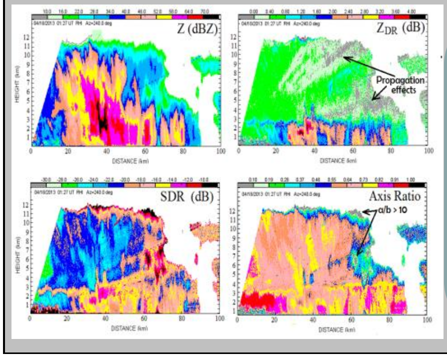

Fig. 4. Same as in Fig. 3 but the data were collected on April 18, 2013 at 0127Z at an azimuth of 240°. Note a strong manifestation of the propagation effects in the Z_{DR} field. The SDR field is almost immune to these effects. Regions with particles having a/b > 10 are indicated with the black arrows. In contrast to Z_{DR} field, SDR and Axis Ratio fields preserve the vertical structure of the thunderstorm. The Axis Ratio field was generated from the SDR field using Fig.2 results.

SDR in radar echoes from insects

Flying insects are aligned and optically strong scatterers in contrast to ice cloud particles. Radar echoes from insects are frequently asymmetric. How does SDR perform in such a medium?

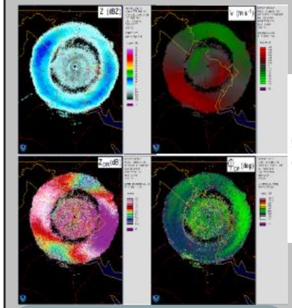

Fig. 5. (left top): The reflectivity field observed with WSR-88D KWLX located in Sterling, VA. The data were collected on 07/07/2012 1208Z at an elevation of 3.7°. (top right, bottom left, and bottom right): Same as in the left top panel but for the radial Dopppler velocity, Z_{DR}, and Φ_{DP}.

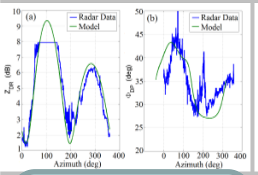

Fig. 6. (a): The azimuthal dependence of Z_{DR} (the blue curve) for the central ring in the outer echo layer in Fig. 5. The green line is the model results based on eq. (3). (b): Same as in (a) but for the differential phase.

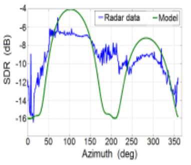

Fig. 7. Values of SDR obtained from radar data (blue line) and modeled data (green curve). A discrepancy at an azimuth near 200° is from ground clutter contamination .

The performance of SDR in radar echoes from insects provides further evidence of the SDR utility for oriented scatterers.

CONCLUSIONS:

- SDR can be used as a parameter to infer particles' axis ratios. It is obtained from Z_{DR} and ρ_{hv} measurements by a polarimetric radar in the STAR mode. SDR values estimated from WSR-88D radar measurements vary in an interval from about -30 dB to approximately -7 dB which corresponds to a wide range of axis ratios (i.e., from very large axis ratio *a/b* ≈10 to almost spherical particles with *a/b* ≈1, see the black and white arrows in Figs. 3 and 4).

- SDR represents a proxy for intrinsic CDR when the phase propagation impacts are effectively removed so SDR is immune to changes in the differential phase (CDR strongly depends on differential phase). SDR depends on differential attenuation but its impact is weaker than that on Z_{DR} (compare Z_{DR} and SDR fields in Fig. 4).

- CDR is measured with radars employing circular polarization. Copolar echoes for such radars are usually weak which limits the range of CDR observations. SDR is estimated from STAR linear polarization measurements which have two strong returns in receiving channels. This results in longer effective distances for SDR observations than those for CDR.

- SDR exhibits a satisfactory performance in echoes from insects, i.e., for aligned scatterers. Insects are optically strong scatterers. Reasonable SDR results for strong aligned scatterers (Fig. 7) make application of SDR more confident for ice particles, which are optically soft scatterers.